ELSEVIER

Polymer 40 (1999) 1403–1409

polymer

Photoinitiated polymerization of a dimethacrylate oligomer: 2. Kinetic studies

L. Lecamp[a], B. Youssef[a], C. Bunel[a,*], P. Lebaudy[b]

[a]*Laboratoire de Matériaux Macromoléculaires, Institut National des Sciences Appliquées de Rouen, Place E. Blondel, BP 08, 76131 Mont Saint Aignan Cédex, France*

[b]*Laboratoire d'Etude et de Caractérisation des Composés Amorphes et des Polymères, UFR des Sciences et Techniques, Université de Rouen, Place E. Blondel, 76821 Mont Saint Aignan, Cédex, France*

Received 21 April 1998; revised 19 May 1998; accepted 19 May 1998

Abstract

The kinetic of photoinitiated polymerization of a dimethacrylate oligomer was studied by using isothermal photocalorimetry. The reaction was realized with 2,2-dimethyl-2-hydroxyacetophenone (Darocur 1173) as radical photoinitiator. Two kinetic models were applied. First, it was shown that an autocatalytic model can describe this reaction in a satisfying way. The reaction temperature does not influence the *m* and *n* orders of the reaction which were found to be constant and respectively equal to 0.8 and 2. The phenomenological rate constant *k* varies with temperature according to the Arrhenius law up to 80°C. Above this temperature, this law can again be checked if the initial variation of double bond concentration due to thermal polymerization is taken into account. In addition, by means of a mechanistic model, the k_p and k_t rate constants were calculated. Their evolution with conversion was studied at 50°C and well illustrates the importance of the reactive diffusion mechanism.

Keywords: Dimethacrylate oligomer; Photocrosslinking; Kinetic

1. Introduction

The photoinitiated polymerization of multifunctional monomers leads to highly crosslinked networks and particular behaviours such as autoacceleration and autodeceleration [1–4], incomplete functional group conversion [5–8], delay in volume shrinkage with respect to equilibrium [9,10], and unequal functional group reactivity [7,11,12]. Moreover, the high rate and the great exothermic effect of this reaction can modify the final polymeric material properties. A better control of the homogeneity can result from a good knowledge of the kinetic behaviour of these multifunctional systems.

The kinetics of photoinitiated polymerization has been the subject of many works [13–18]. Kinetic models result in the evolution of reactive species concentration as a function of time by means of a reaction rate expression. Generally, kinetic models are phenomenological or mechanistic. Because of the complex nature of the photoinitiated polymerization, phenomenological models are often used to describe these systems. However, these models have been originally conceived for reactions of which rates are only controlled by the chemical reaction. Thus, the autocatalytic model has been much used to predict the treatment of thermosetting resins [29,30]. On the other hand, very few works put forward the use of these models for the photopolymerization kinetic. Indeed, these reactions are controlled by reaction diffusion as a termination mechanism [2,6,19–24]. By this reaction diffusion mechanism, the mobility of the radical species takes place through unreacted functional groups until they encounter a second radical for a termination step. Thus, the reaction diffusion is a propagating termination mechanism. This mechanism is physically different from the termination mechanism by segmental or translational diffusion which implies the diffusion of macroradicals and chain segments to move radicals within a reaction zone before termination. Those are related to a diffusion polymer coefficient whereas the reactive diffusion is related to the kinetic propagation constant. Thus, other models taking this phenomenon into account are preferred to describe the photochemical reactions.

In a previous work [25], we have studied the photoinitiated polymerization of a dimethacrylate oligomer with 2,2-dimethyl-2-hydroxyacetophenone (Darocur 1173) as

* Corresponding author.

0032-3861/98/$ - see front matter
PII: S0032-3861(98)00380-2

radical photoinitiator by using isothermal photocalorimetry. The effect of temperature was particularly investigated. We have shown that a maximum conversion was obtained at temperatures near 90°C. Below 90°C, the photochemical reaction completely stops when the glass transition temperature of the crosslinked material is reached. Thus, conversion increases with reaction temperature. On the other hand, for temperatures higher than 90°C, our experimental conditions allow thermal polymerization to occur before irradiation. Thus, photochemical conversion decreases when reaction temperature increases.

In this paper, we use the results of this previous study to describe the kinetic of this photocrosslinking reaction. The first part is dedicated to a phenomenological model. In the second part, we use a mechanistic model in order to determine the different kinetic rate constants of the above system.

2. Experimental

2.1. Materials

The chemical formula of the reactant used is the following:

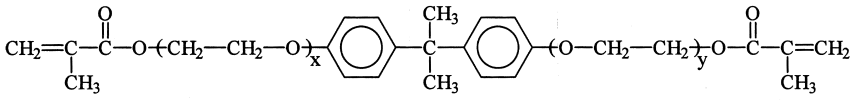

n = x + y = 4.8

The average number of oxyethyl units in the dimethacrylate oligomer (Akzo, $M = 575$ g mol^{-1}) was determined by ^{1}H n.m.r. analysis and was found to be equal to 4.8.

The photoinitiator 2,2-dimethyl-2-hydroxyacetophenone (Darocur 1173: 0.15% (w/w) i.e. 10^{-2} mol l^{-1}) was dissolved in the oligomer under stirring at room temperature for 3 h.

2.2. Measurement

The photocrosslinking reaction kinetics were monitored by a differential scanning calorimeter (DSC 7 Perkin Elmer) topped by an irradiation unit. Heat flow versus time was recorded in isothermal mode under nitrogen atmosphere. The optical part of the calorimeter, the sample preparation, the treatment of the thermogram and the computation of conversion and reaction rate were described elsewhere [25]. The UV radiation intensity was measured at the sample level by a radiometer at 365 nm and was 2.7 mW cm^{-2}.

Photoinitiated polymerizations evolve an important thermal effect and kinetic constants are very sensitive to an increase in temperature. A simulation of heat transfer within monomer film during photocrosslinking allows us to show that our experimental conditions (thin film of 0.2 mm, reaction rate not too fast) are convenient to work in isothermal conditions [26]. Indeed, the elevation of temperature within the film is always lower than 1°C.

3. Results and discussion

3.1. Phenomenological model

Generally, phenomenological models are based on two kinetic relations [27–30]. For the *n*th order reaction, the reaction is directly proportional to the unreacted monomer concentration according to Eq. (1):

$$\frac{dC}{dt} = k(1-C)^n \tag{1}$$

where C is the relative conversion, k is the rate constant and n is the order of reaction. For an autocatalytic reaction, one of the products of the reaction markedly increases the reaction rate. The kinetic of this reaction can be expressed as following:

$$\frac{dC}{dt} = kC^m(1-C)^n \tag{2}$$

where m is the autocatalytic exponent. The rate constant k is usually assumed to observe the Arrhenius law:

$$k = A e^{-\frac{E}{RT}} \tag{3}$$

where A is a pre-exponential factor and E is the activation energy.

The later model is usually used to describe the kinetics of autocatalytic reactions which are characterized by a maximum reaction rate between 20 and 40% conversion. The shape of the photoinitiated polymerization rate curves is the same as the autocatalytic reaction (Fig. 1). Although photoinitiated polymerization is autoaccelerated and not autocatalyzed, this model can be applied to describe these reactions in a purely mathematical way.

DSC thermograms give dH/dt versus time. The relative conversion C is defined as the ratio $\Delta H_t/\Delta H_p$ or S_1/S (Fig. 2), where ΔH_t is the polymerization enthalpy at t (area S_1) and ΔH_p is the overall polymerization enthalpy at a given temperature (area S). Thus,

$$\frac{dC}{dt} = \frac{1}{\Delta H_p}\frac{dH}{dt}$$

and Eq. (2) can then be written:

$$\frac{dC}{dt} = k\left(\frac{S_1}{S}\right)^m\left(\frac{S_2}{S}\right)^n \tag{4}$$

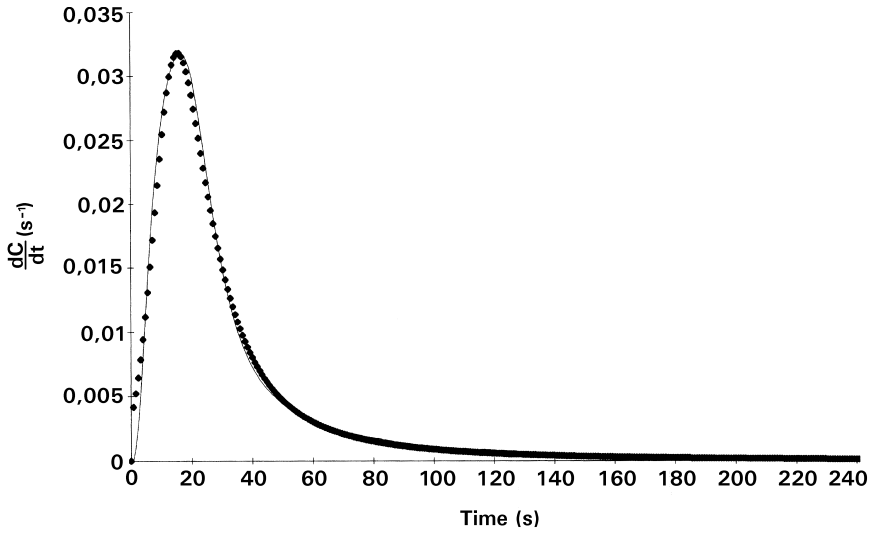

Fig. 1. Typical photoinitiated polymerization rate curve versus time at 50°C. Experimental curve (——) and modelization (♦).

Some studies were realized on the dependence of the orders *m* and *n* on these factors [31–34]. Indeed, both *m* and *n* orders may change greatly with temperature, surrounding atmosphere and the type of functionality.

In this work, we have investigated the effect of temperature on *m*, *n* and *k* values. The kinetics of photoinitiated polymerization were followed over a wide temperature range (30–160°C) under nitrogen atmosphere.

Eq. (2) leads to Eq. (5) and the plot of log d*C*/d*t* versus log[$C^{m/n}$(1-*C*)] must be a linear relation (Fig. 3) by adjusting the ratio *m*/*n*, which is first estimated as S_1/S_2 on both sides of peak apex. The zero ordinate gives *k* and the slope *n* allows one to calculate *m*.

$$\log \frac{dC}{dt} = \log k + n \log [C^{m/n}(1-C)] \tag{5}$$

The calculated exponents *m* and *n* are constant and equal to 0.8 and 2 whatever the temperature. The rate constant *k* only varies with temperature. Thus, the equations of the model are:

$$\frac{dC}{dt} = kC^{0.8}(1-C)^2 \text{ or } \frac{dC}{dt} = k\left(\frac{S_1}{S}\right)^{0.8}\left(\frac{S_2}{S}\right)^2 \tag{6}$$

To check the validity of this model, we have compared experimental and modelized results. In order to obtain an expression of the conversion versus time, it a priori seems easier to integrate Eq. (6). Unfortunately, this integration is very complex and we have chosen to realize a numerical treatment. For this computation, we consider that, on a very small time increment, conversion increases with time according to a linear relation of which the slope is given by:

$$\frac{dC_{i+1}}{dt} = \frac{C_{i+1}-C_i}{t_{i+1}-t_1} = \frac{C_{i+1}-C_i}{\Delta t} \tag{7}$$

Generally, the fit between the model and experimental rate is good for all the temperatures (e.g. on Fig. 1 at 50°C).

Likewise, simulated and experimental relative

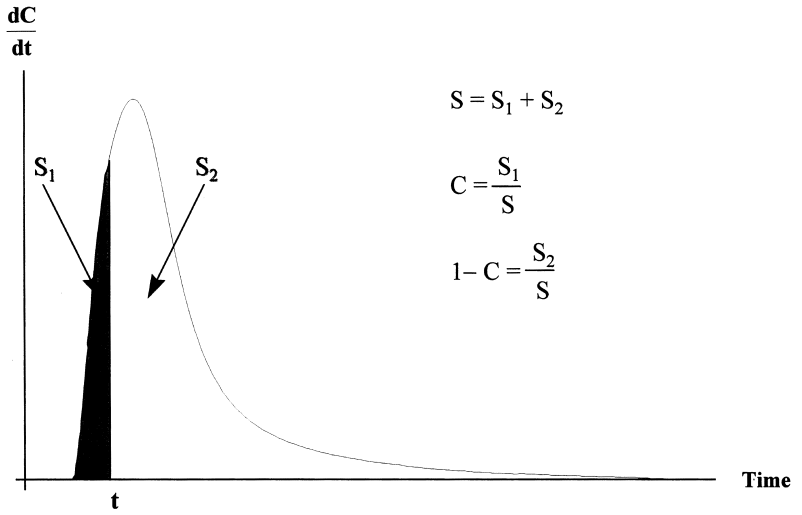

$$S = S_1 + S_2$$

$$C = \frac{S_1}{S}$$

$$1 - C = \frac{S_2}{S}$$

Fig. 2. Relation between relative conversion and partial areas.

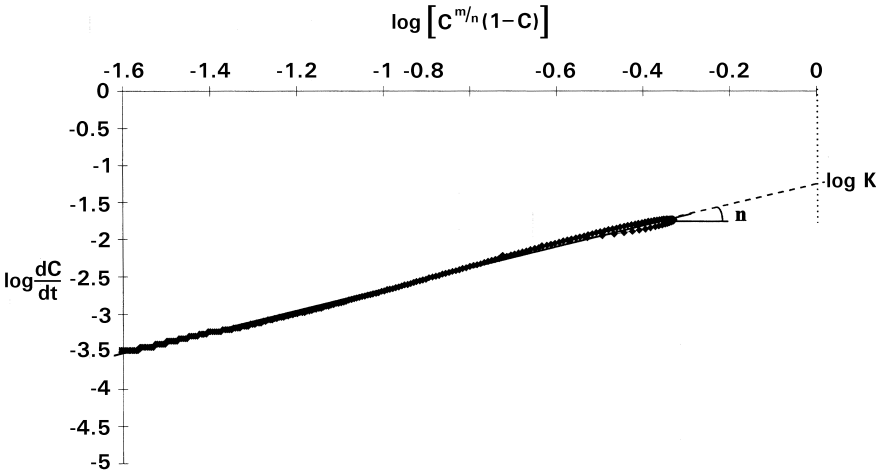

Fig. 3. Determination of *m*, *n* and *k* values.

conversions or absolute conversions (*Y*%) are in good agreement (e.g. *Y*% versus time at different temperatures; Fig. 4). *Y*% is defined as $100\Delta H_t/\Delta H_0^{theor}$ (or $100(S_1/S_0)$) where ΔH_0^{theor} is the theoretical enthalpy (-13.1 kcal mol^{-1} per methacrylate double bond[40], i.e. -190 J/g for our dimethacrylate oligomer) which corresponds to an area S_0.

The plot *lnk* versus $1/T$ (Fig. 5; full symbol) shows that *k* linearly increases up to 80°C; the slope gives a small activation energy of 2.2 kcal mol^{-1}.

Above 80°C, *k* decreases because of thermal polymerization already mentioned in our first paper [25]. Indeed, in Eq. (4), only the double bond able to react (area *S*) is considered. Thus, to take into account the double bond consumed by thermal polymerization before irradiation above 80°C, we have estimated a fictitious area $S' = Y\%S_0/100$ by extrapolation of the absolute conversion versus temperature, which can be assumed as a straight line (Fig. 6). One can see that above 80°C, S' is rapidly equal to S_0 (*Y*%∼100 at 110°C).

Thus, introducing S', Eq. (6) becomes:

$$\frac{dC}{dt} = \frac{k}{\left(\frac{S}{S'}\right)^{2.8}}\left(\frac{S_1}{S'}\right)^{0.8}\left(\frac{S_2}{S'}\right)^{2} \tag{8}$$

This relation reveals a new corrected rate constant k_{corr}:

$$k_{corr} = \frac{k}{\left(\frac{S}{S'}\right)^{2.8}} \tag{9}$$

This new rate constant can be calculated as soon as thermal polymerization appears, i.e. above 80°C. The *k* values are reported in Fig. 5 (open symbol) and now fit very well the Arrhenius straight line.

3.2. Mechanistic model

Many researchers have integrated the reaction diffusion

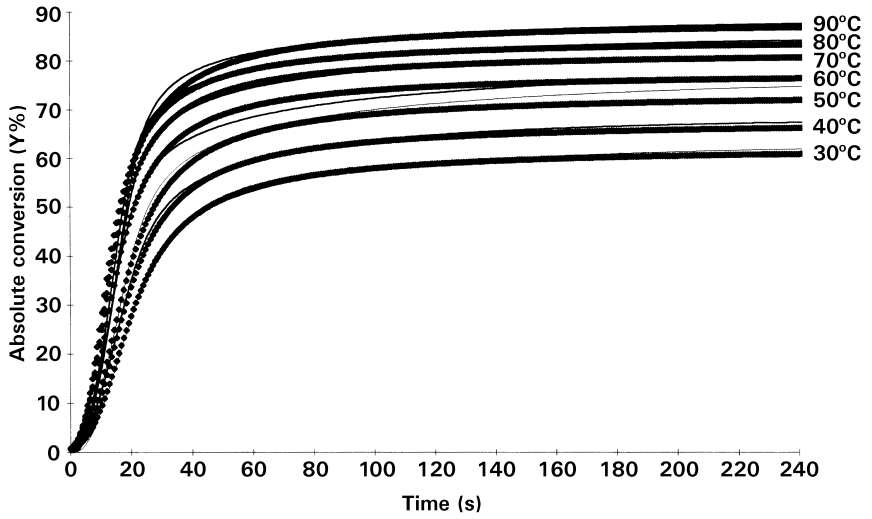

Fig. 4. Comparison between experimental (——) and modeled (♦) conversion curves at different temperatures.

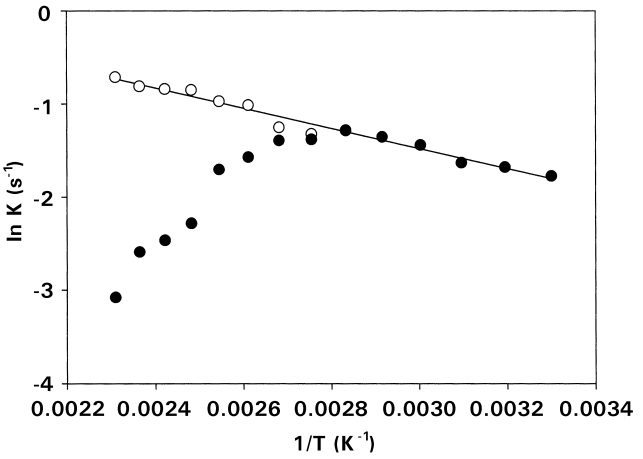

Fig. 5. Temperature dependence of the experimental reaction rate constant k (●) and corrected rate constant k_{corr} (○).

concept to conceive a kinetic model [35,36]. The model we have applied was first revealed by Tryson and Shultz [37] and then developed by Decker et al. [38,39] and Anseth et al. [24,40,41]. This model analyses a series of non-steady state kinetic experiments and allows one to calculate the propagation and termination rate constants.

The model is based on the classical chemical equations of initiation and propagation and only assumes a bimolecular termination:

Initiation:

$$A_2 \xrightarrow{h\nu} 2A^{\bullet} \qquad R_i = 2,3\phi\varepsilon I_0[A_2] \tag{10}$$

$$A^{\bullet} + M \rightarrow AM^{\bullet} \qquad [A_2] = [A_2]_0 e^{-2,3\phi_0\varepsilon I_0 t} \tag{11}$$

Propagation:

$$-M^{\bullet} + M \xrightarrow{k_p} -MM^{\bullet} \quad R_p = -\frac{d[M]}{dt} = k_p[M^{\bullet}][M] \tag{12}$$

Bimolecular termination:

$$-M^{\bullet} + {}^{\bullet}M - \xrightarrow{k_t} -MM- \quad R_t = -\frac{d[M^{\bullet}]}{dt} = 2k_t[M^{\bullet}]^2 \tag{13}$$

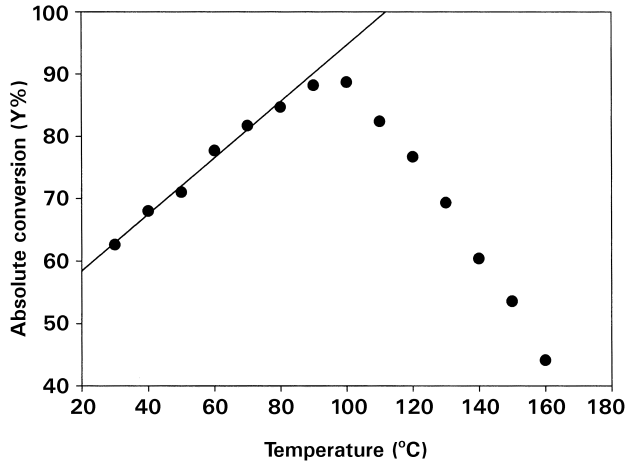

Fig. 6. Absolute conversion (Y%) versus temperature.

where R_i, R_p, R_t are respectively the initiation, propagation and termination rates, k_p and k_t are respectively the propagation and termination rate constants, ϕ is the initiation quantum yield, ϕ_0 is the number of radicals produced per absorbed light energetic quanta, ε is the molar extinction coefficient, I_0 is the light intensity, $[A_2]$ and $[M]$ are respectively the photoinitiator and monomer concentrations.

Notice that, for the best understanding of the kinetic behaviour, it is easier to work at low temperatures to avoid thermal polymerization.

In order to determine k_p and k_t, the first step is to follow the polymerization rate as a function of time under continuous irradiation. In our case, from DSC experiments, R_p is defined as

$$R_p = \frac{[M]_0}{\Delta H_0^{theor}} \frac{dH}{dt}$$

At low photoinitiator concentration and assuming a quasi-steady state for $[M^{\bullet}]$, the evolution of $k_p/k_t^{1/2}$ can be expressed by:

$$\frac{k_p}{k_t^{1/2}} = \frac{R_p}{[M]} \sqrt{\frac{2,3\phi\varepsilon I_0[A_2]}{2}} \tag{14}$$

As Anseth et al. [24,41], no attempts were made to measure the initiation quantum yield (ϕ). Therefore, it is the variation of $\phi^{1/2}(k_p/k_t^{1/2})$ for different reaction temperatures which is plotted in Fig. 7. At the beginning of the reaction, the high increase in viscosity reduces the segmental or translational diffusion of the reactive species and the collision between two radicals is more and more difficult. k_t decreases faster than k_p and $k_p/k_t^{1/2}$ increases. Then, the termination mechanism becomes reaction diffusion controlled and can be assimilated to a propagation mechanism. From the top of the curve and because of the great decrease in the mobility of species, propagation and termination constants and then $k_p/k_t^{1/2}$ decreases quickly.

In a second step, the UV irradiation was cut at a different time of reaction and the reaction rate was monitored during the dark period. Assuming a non-steady state, k_t can be calculated from the integration of Eq. (13):

$$-\frac{d[M^{\bullet}]}{[M^{\bullet}]^2} = 2k_t dt \tag{15}$$

$$\int_{t_0}^{t_1} -\frac{d[M^{\bullet}]}{[M^{\bullet}]^2} = 2k_t \int_{t_0}^{t_1} dt \tag{16}$$

then

$$\frac{1}{[M^{\bullet}]_{t_1}} - \frac{1}{[M^{\bullet}]_{t_0}} = 2k_t(t_1 - t_0) \tag{17}$$

where t_0 is the end of the irradiation period and t_1 is some time later at the beginning of the dark period.

By substituting $[M^{\bullet}] = R_p/k_p[M]$ from Eq. (12) into

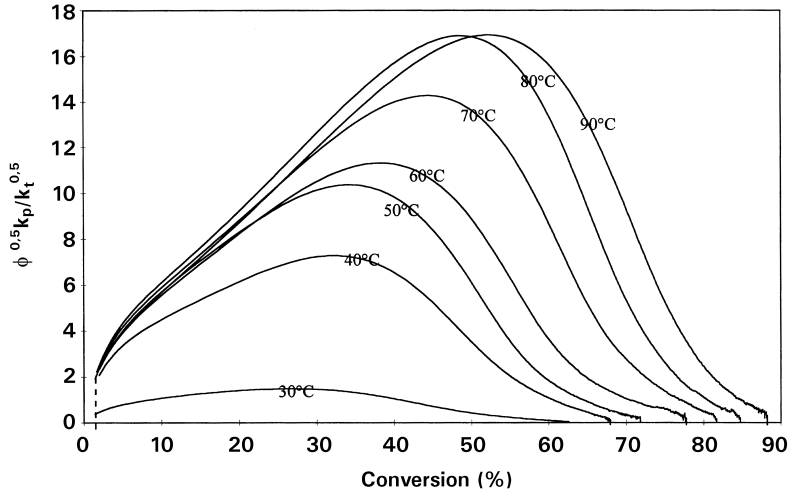

Fig. 7. Variation of $\phi^{1/2}(k_p/k_t^{1/2})$ versus conversion for different reaction temperatures.

Eq. (17), k_t can be calculated as follows:

$$\frac{k_p[M]_{t_1}}{R_{p_{t_1}}} - \frac{k_p[M]_{t_0}}{R_{p_{t_0}}} = 2k_t(t_1 - t_0) \tag{18}$$

i.e.

$$k_t^{1/2} = \frac{k_p/k_t^{1/2}}{2(t_1 - t_0)}\left(\frac{[M]_{t_1}}{R_{p_{t_1}}} - \frac{[M]_{t_0}}{R_{p_{t_0}}}\right)$$

or

$$\phi^{1/2}k_t^{1/2} = \frac{\phi^{1/2}(k_p/k_t^{1/2})}{2(t_1 - t_0)}\left(\frac{[M]_{t_1}}{R_{p_{t_1}}} - \frac{[M]_{t_0}}{R_{p_{t_0}}}\right) \tag{19}$$

This analysis assumes that the kinetic rate constants do not vary during the time increment $(t_1 - t_0)$ where the conversion variation is small. Our experimental conditions allows us to use a very small time increment of 0.8 s. Thus, the conversion change between t_0 and t_1 does not exceed 2%.

One can notice that these calculated constants are average values, i.e. all the double bonds are assumed to have the same reactivity.

The computation of k_p and k_t was carried out at 50°C. The values of $[M]$, R_p at t_0 and t_1 were directly obtained from the DSC thermogram. The variations of ϕk_p and ϕk_t are plotted in Fig. 8.

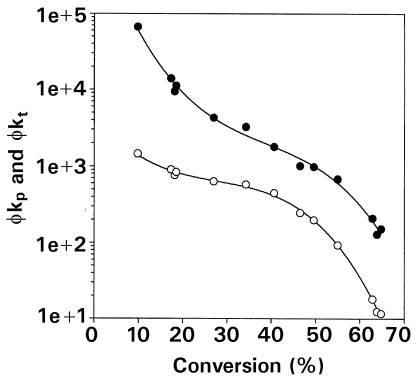

Fig. 8. Variation of ϕk_p and ϕk_t versus conversion at 50°C.

This figure illustrates well the dependence between rate constants and conversion. Generally, termination is controlled by the polymer diffusion whereas propagation is controlled by small monomer molecules. At the beginning of the reaction, the diffusivity of the species decreases with the increase in double bond conversion and explains the rapid drop of k_t. On the other hand, diffusion of the small molecules is not disturbed and k_p is relatively constant. These variations in k_t and k_p lead to the autoacceleration behaviour which characterizes these multifunctional systems. Between 25 and 35% conversion, when the system approaches the gel point, termination becomes reaction diffusion controlled and an inflexion of the k_t curve at 35–40% conversion is observed. Above conversion, propagation becomes monomer and polymer diffusion controlled. k_p and then k_t decrease and quickly tend towards 0. Indeed, at 50°C, the glassy state is reached at about 70% conversion. The lack of mobility of reactive species quickly leads to the end of the photopolymerization reaction.

Moreover, we can notice that our k_p and k_t curves exhibit the same shape as those found by Anseth et al. [24], who also observed a slight variation of these constants versus temperature for a diethyleneglycol dimethacrylate.

4. Conclusion

In this work, we have shown that the kinetics of photoinitiated polymerization can be described either by an autocatalytic model or by a mechanistic model. The first consists of a mathematical description. The effect of temperature is revealed in the variation of the constant rate *k*. *k* follows an Arrhenius law up to 80°C. Above this temperature, this law can be again checked if thermal polymerization, occurring before irradiation, is taken into account. The second model is based on the reaction diffusion concept. A series

of non-steady state analyses allows us to determine the variation of propagation and termination rate constants during the course of the reaction. The results show well the dependence of the rate constants on the reaction diffusion as a termination mechanism.

References

[1] Allen P, Simon G, Williams D, Williams E. Macromolecules 1989;22:809.
[2] Cook WD. Polymer 1992;33:2152.
[3] Broer DJ, Mol GN, Challa G. Polymer 1991;32 (6):690.
[4] Kloosterboer JG, Lijten GFCM, Boots HMJ. Makromol Chem Makromol Symp 1989;24:223.
[5] Doornkamp AT, Tan YY. Polym Commun 1990;31:362.
[6] Anseth KS, Newman SM, Bowman CN. Adv Polym Sci 1995;122:177.
[7] Kloosterboer JG. Adv Polym Sci 1988;84:1.
[8] Allen P, Bennet D, Hagias S, Hounslow A, Ross G, Simon G, Williams D, Williams E. Eur Polym J 1989;25:785.
[9] Bowman CN, Peppas NA. Macromolecules 1991;124:1914.
[10] Kloosterboer JG, van de Hei GMM, Gossink RG, Dortant GCM. Polym Commun 1984;25:322.
[11] Kloosterboer JG, van de Hei GMM, Boots HMJ. Polym Commun 1984;25:354.
[12] Bowman CN, Peppas NA. Chem Eng Sci 1992;47:1411.
[13] Stickler M, Panke D, Hamielec AE. J Polym Sci Polym Chem 1984;22:2243.
[14] Kurdikar DL, Peppas NA. Macromolecules 1994;27:4084.
[15] Kurdikar DL, Peppas NA. Macromolecules 1994;27:733.
[16] Achilias DS, Kiparissides C. Macromolecules 1992;25:3739.
[17] Kurdikar DL, Somvarsky J, Dusek K, Peppas NA. Macromolecules 1995;28:5910.
[18] Buback M, Huckestein A, Russell GT. Macromol Chem Phys 1994;195:539.
[19] Ballard MJ, Napper DH, Gilbert RG. J Polym Sci Polym Chem 1986;24:1027.
[20] Zhu S, Tian Y, Hamielec AE, Eaton DR. Macromolecules 1990;23:1144.
[21] Soh SK, Sundberg DC. J Polym Sci Polym Chem 1982;20:1345.
[22] Stickler M. Makromol Chem 1983;184:2563.
[23] Cook WD. J Polym Sci Polym Chem 1993;31:1053.
[24] Anseth KS, Wang CM, Bowman CN. Polymer 1994;35:3243.
[25] Lecamp L, Youssef B, Bunel C, Lebaudy P. Polymer 1997;38 (25):6089.
[26] Lecamp L, Youssef B, Bunel C, Lebaudy P. J Thermal Anal 1998;51:889.
[27] Waters DN, Paddy JL. Anal Chem 1988;60:53.
[28] Chandra R, Soni K. Polym Int 1993;31:239.
[29] Chandra R, Soni K. Proc Polym Sci 1994;19:137.
[30] Stutz H, Mertes J, Neubecker K. J Polym Sci Polym Chem 1993;31:1879.
[31] Andrzejewska E. Polymer 1996;37:1039.
[32] Andrzejewska E. Polymer 1996;37:1047.
[33] Andrzejewska E, Linden L-A, Rabek J-F. Polym Int 1997;42:179.
[34] Lecamp L, Vaugelade C, Youssef B, Bunel C. Eur Polym J 1997;33 (9):1453.
[35] Tulig JT, Tirrell M. Macromolecules 1981;14:1501.
[36] Russell GT, Napper DH, Gilbert RG. Macromolecules 1988;21:2133.
[37] Tryson GR, Shultz AR. J Polym Sci Polym Phys Ed 1979;17:2059.
[38] Decker C, Moussa K. Eur Polym J 1990;26:393.
[39] Decker C, Elzaouk K, Decker D. JMS-Pure Appl Chem 1996;A33 (2):173.
[40] Anseth KS, Bowman CN, Peppas NA. J Polym Sci Polym Chem 1994;32:139.
[41] Anseth KS, Kline LM, Walker TA, Anderson KJ, Bowman CN. Macromolecules 1995;28:2491.